

Properties of bulk scandium nitride crystals grown by physical vapor transport

Cite as: Appl. Phys. Lett. **116**, 132103 (2020); <https://doi.org/10.1063/1.5141808>

Submitted: 09 December 2019 . Accepted: 18 March 2020 . Published Online: 01 April 2020

Hayder Al-Atabi , Qiye Zheng , John S. Cetnar , David Look, David G. Cahill , and James H. Edgar 



[View Online](#)



[Export Citation](#)



[CrossMark](#)

ARTICLES YOU MAY BE INTERESTED IN

[High mobility and high thermoelectric power factor in epitaxial ScN thin films deposited with plasma-assisted molecular beam epitaxy](#)

Applied Physics Letters **116**, 152103 (2020); <https://doi.org/10.1063/5.0004761>

[Molecular beam epitaxy and characterization of wurtzite \$Sc_xAl_{1-x}N\$](#)

Applied Physics Letters **116**, 151903 (2020); <https://doi.org/10.1063/5.0002445>

[Ultrafast dynamics of hole self-localization in \$\beta\$ -Ga₂O₃](#)

Applied Physics Letters **116**, 132101 (2020); <https://doi.org/10.1063/5.0003682>

Lock-in Amplifiers
up to 600 MHz



Properties of bulk scandium nitride crystals grown by physical vapor transport

Cite as: Appl. Phys. Lett. **116**, 132103 (2020); doi: 10.1063/1.5141808

Submitted: 9 December 2019 · Accepted: 18 March 2020 ·

Published Online: 1 April 2020



Hayder Al-Atabi,^{1,2} Qiyue Zheng,³ John S. Cetnar,⁴ David Look,^{4,5} David G. Cahill,³ and James H. Edgar^{1,a}

AFFILIATIONS

¹Tim Taylor Department of Chemical Engineering, Kansas State University, Manhattan, Kansas 66506, USA

²Chemical Engineering Department, The University of Technology, PO Box 35010, Baghdad, Iraq

³Department of Materials Science and Engineering, University of Illinois at Urbana-Champaign, Urbana, Illinois 61801, USA

⁴Sensors Directorate, Air Force Research Laboratory, WPAFB, Ohio 45433, USA

⁵Semiconductor Research Center, Wright State University, Dayton, Ohio 45435, USA

^aAuthor to whom correspondence should be addressed: edgarjh@ksu.edu

ABSTRACT

In this study, the growth of scandium nitride (100) single crystals with high electron mobility and high thermal conductivity was demonstrated by physical vapor transport (PVT). Single crystals were grown in the temperature range of 1900 °C–2140 °C under a nitrogen pressure between 15 and 20 Torr. Single crystal tungsten (100) was used as a nearly lattice constant matched seed crystal. Growth for 20 days resulted in a 2 mm thick crystal. Hall-effect measurements revealed that the layers were *n*-type with a 300 K electron concentration and a mobility of $2.17 \times 10^{21} \text{ cm}^{-3}$ and $73 \text{ cm}^2/\text{V s}$, respectively. Consequently, this ScN crystal had a low electrical resistivity, $3.94 \times 10^{-5} \Omega \text{ cm}$. The thermal conductivity was in the range of 51–56 W/m K, three times higher than those in previous reports for ScN thin films. This study demonstrates the viability of the PVT crystal growth method for producing high quality bulk scandium nitride single crystals.

Published under license by AIP Publishing. <https://doi.org/10.1063/1.5141808>

Scandium nitride (ScN) is a group III(B)–V semiconductor with a rock salt crystal structure.^{1–4} There is increasing interest in ScN owing to its wide range of potential applications including thermoelectrics,^{5–8} inclusion as a semiconducting component in epitaxial single crystalline nitride metal/semiconductor superlattices,⁹ spintronics,¹⁰ piezoelectrics,^{11,12} application as an interlayer for the growth of high quality GaN based devices¹³ with reduced dislocation densities,¹⁴ and for tuning the optical gaps of IIIa nitrides by alloying.^{15,16}

ScN has an indirect energy bandgap of approximately 0.9 eV, and its optical gap expands as the electron concentration increases and fills the lower part of the conduction band.¹⁷ Unintentional oxygen doping usually occurs even under high vacuum conditions due to the high affinity of Sc for oxygen, and so its electron concentration is often in the degenerate range (10^{20} – 10^{22} cm^{-3}).^{5,7,18}

Scandium nitride is typically produced in thin film forms (<1 μm) by standard techniques such as molecular beam epitaxy,^{19,20} hydride vapor phase epitaxy (HVPE),^{21,22} and sputtering.^{5,23} The deposition temperature in these techniques is generally 1000 °C or less. The resulting thin films produced by these techniques generally have small grain sizes, which can compromise the

electrical and thermal properties due to charge and phonon scattering by grain boundaries.

The quality of ScN is frequently assessed by electrical property measurements. Dismukes *et al.*²⁴ demonstrated a carrier concentration and Hall mobility of approximately $1 \times 10^{20} \text{ cm}^{-3}$ and $150 \text{ cm}^2/\text{V s}$, respectively, at 300 K in ScN films grown on sapphire by HVPE. Their Hall-effect measurements suggested that ScN would have a higher electron mobility if the carrier concentration were reduced. Later, several studies were conducted to investigate the carrier concentration, Hall mobility, and electrical resistivity of ScN thin films grown by different methods. Sputter-deposited thin films of ScN by Gregoire *et al.*²⁵ demonstrated a high carrier concentration and Hall mobility of $1\text{--}3 \times 10^{21} \text{ cm}^{-3}$ and $20\text{--}100 \text{ cm}^2/\text{V s}$, respectively. MBE-grown ScN thin films by Ohgaki *et al.*²⁶ exhibited a carrier concentration in the range of $10^{19}\text{--}10^{21} \text{ cm}^{-3}$ with the Hall mobility varying from 10 to $150 \text{ cm}^2/\text{V s}$. Most recently, Casamento *et al.*²⁷ reported a carrier concentration of $1.05 \times 10^{20}\text{--}1.55 \times 10^{20} \text{ cm}^{-3}$ and a Hall mobility of $11\text{--}23 \text{ cm}^2/\text{V s}$, respectively, for ScN thin films on GaN and AlN substrates. A low electrical resistivity of $100\text{--}600 \mu\Omega \text{ cm}$ at room temperature was demonstrated for ScN films grown by MBE.²⁸

The thermal properties of ScN have also been previously measured to assess its quality. Burmistrova *et al.*⁵ reported a room temperature thermal conductivity of $20.7 \text{ W m}^{-1} \text{ K}^{-1}$ for an epitaxial ScN thin film grown by the sputtering method. Recently, Kerdpongpanya *et al.*²⁹ have described a theoretical model based on *ab initio* calculations taking into consideration the effect of the ScN crystal grain size. The model showed that the thermal conductivity decreases as the ScN layer thickness and grain size decrease due to the smaller phonon mean free path allowed for transport.

In this work, bulk ScN (100) single crystals were produced for thermal conductivity and Hall effect measurements by the sublimation method, also known as physical vapor transport (PVT), which employs much higher temperatures, $>1750^\circ\text{C}$, than thin film deposition methods. Consequently, the molecular nitrogen reactivity is greater and the adatom diffusion rates are higher with this technique, which may help to reduce the defect densities in the ScN crystal in comparison to thin film deposition methods. Furthermore, PVT can produce thick ScN free-standing crystals for subsequent measurements of their electrical and thermal properties. The crystal was formed from the sublimation of a scandium nitride source at high temperatures ($>1750^\circ\text{C}$) to produce a scandium vapor in a background of nitrogen gas. We previously demonstrated that such thick ScN crystals have a much narrower x-ray diffraction peak width than what has been reported for thin films.³⁰

The ScN crystal growth was carried out in a tungsten heating element furnace that has a maximum temperature of 2400°C . Tungsten previously proved to be an unreactive metal for the sublimation growth of ErN³¹ and TiN,³² so it was used as a seed for the ScN crystal, and to manufacture crucibles and lids used in the experiments. Because of its high melting temperature ($>3000^\circ\text{C}$), tungsten substrates can withstand much higher temperatures than what is possible with standard substrates such as silicon, sapphire, or silicon carbide. A single crystal tungsten seed with a (100) orientation was used. In this orientation, the room temperature lattice constant mismatch between tungsten and ScN is only 0.3%.³⁰ The ScN source was synthesized by heating small chunks of pure Sc metal (99.9% purity) in ultra-high-purity nitrogen at 1100°C and 500 Torr for 10 h. The sublimation was carried out at the temperature range of 1900°C – 2140°C under a nitrogen pressure between 15 and 20 Torr. The growth time was up to 20 days.

The thermal conductivity of the ScN crystal was measured by time-domain thermal reflectance (TDTR).^{33–36} Prior to the measurement, the sample was cleaned by ultrasonication in ethanol, and coated with an Al transducer layer with a thickness of approximately 80 nm by magnetron sputtering.

The ratio of the in-phase (V_{in}) and out-of-phase (V_{out}) signal from the lock-in amplifier was fit to a thermal diffusion model obtained from an analytical solution for heat flow in a layered structure based on Fourier's law.³³ The diffusive thermal transport model used for TDTR data fitting included parameters for thermal conductivity, heat capacity, and thickness of the Al transducer layers and the ScN sample as well as the Al/ScN interface thermal conductance. The heat capacity of ScN was taken from a prior first-principles calculation.³⁷ Since the ScN sample studied by TDTR had dimensions much thicker than the maximum TDTR thermal penetration depth $d_p = \sqrt{\Lambda / (\pi f C_p)} \approx 0.8 \mu\text{m}$ (where Λ is the ScN thermal conductivity), the sample boundaries were not detected and they were treated as semi-infinite bulk.

Temperature-dependent Hall-effect measurements were carried out on a LakeShore 7507 system over a temperature range 7–320 K. The magnetic-field strength was 10 kG, the maximum available, and the current was 100 mA, also a maximum. The ScN sample was mounted on a thin slab of BeO (high thermal conductivity) and indium contacts were carefully applied on the corners of the sample with a soldering iron. The Hall-effect data were analyzed by applying the van der Pauw equations, giving resistivity ρ , mobility μ , and carrier concentration n vs temperature T .³⁸

The physical vapor transport method produced bulk ScN crystals with (100) orientation and thicknesses up to 2 mm as shown in Fig. 1. There are large steps on the crystal surface due to step bunching and faceting occurring during crystal growth, a consequence of strain and threading dislocations. Step bunching is caused by a difference between the surface diffusion distance and the distance of neighboring kinks. In the case of step formation, the average distance between neighboring kinks is far smaller than the average distance of surface diffusion of the adatoms. Fourfold symmetry features appear on the surface as a characteristic of the (100) plane on the rock salt crystal structure. Measurements were taken on free-standing pieces of ScN that cracked off the tungsten seed.

Hall-effect measurements revealed that the ScN layers were *n*-type and showed that at 7 K, the resistivity (ρ) was $1.42 \times 10^{-5} \Omega \text{ cm}$, one of the lowest resistivity values ever measured in a semiconducting material; also, $\mu \approx 2 \times 10^2 \text{ cm}^2/\text{V s}$ and $n \approx 2 \times 10^{21} \text{ cm}^{-3}$. The n and μ data were noisy, because with a sheet resistance of only $2 \times 10^{-3} \Omega/\text{sq}$, the Hall voltages, even at a current of 100 mA, were extremely small. Fortunately, the charge carriers were highly degenerate, so we can assume that n is constant with temperature. This view is supported by many studies in the literature, including those of Cetnar *et al.*¹⁸ A smoothed version of n vs T , and also a least squares fit of n vs T , are shown in Fig. 2. The fit gives $n\text{-avg} = 2.17 \times 10^{21} \text{ cm}^{-3}$. Also, shown in this figure are the raw data of ρ vs T , displaying a much better S/N ratio than either n or μ vs T . From the ρ vs T and the $n\text{-avg}$ results, an accurate μ vs T curve was obtained from $\mu = (e \times n\text{-avg} \times \rho)^{-1}$. Note that ρ , μ , and n vs T , all show the classical shape of metallic-type conduction, in which n is flat, ρ increases monotonically, and μ decreases



FIG. 1. Photograph of the 2 mm thick ScN layer on a 9 mm diameter W (100) substrate.

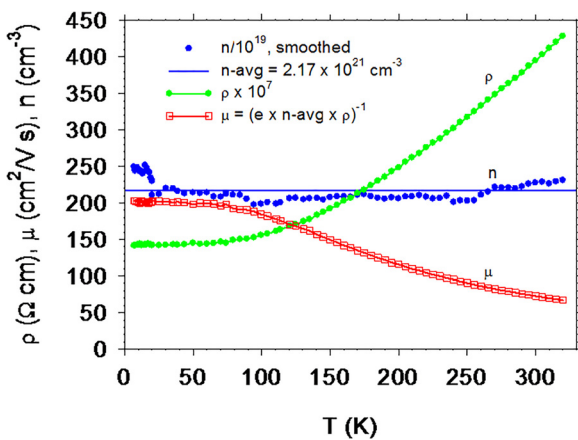


FIG. 2. Hall-effect measurements of bulk ScN crystals.

monotonically. At low temperatures, say $T < 50$ K, the ionized donors dominate the scattering, although there is a slight contribution from acoustic phonons. Then, at higher temperatures, optical phonons become much more important and eventually dominate the scattering. Finally, using previously published methodology,³⁹ we can use n and μ at low temperature to determine the bulk ScN donor and acceptor concentrations, which are $N_D = 2.9 \times 10^{21}$ and $N_A = 5.7 \times 10^{20} \text{ cm}^{-3}$.

At 300 K from Fig. 2, the electron concentration and mobility were $\approx 2.2 \times 10^{21} \text{ cm}^{-3}$ and $73 \text{ cm}^2/\text{V s}$, respectively. Consequently, these ScN crystals had a low electrical resistivity, $3.9 \times 10^{-5} \Omega \text{ cm}$. Sc has a high affinity for oxygen, and is likely the main impurity, arising from the background oxygen during the growth process, and producing the degenerate electron concentration.^{5,7,18} Unintentional oxygen doping shifts the Fermi energy into the conduction band while keeping the density of states of ScN the same. Consequently, the carrier concentration and electrical conductivity are increased. Assuming the dominant charge carrier scattering is by ionized donors, this suggests that the electron mobility in lightly doped ScN would be significantly higher.

The thermal conductivity (Λ) of ScN crystals was measured at room temperature. A representative TDTR data and model fitting are shown in Fig. 3. The average thermal conductivity (Λ) was $54 \pm 3 \text{ W m}^{-1} \text{ K}^{-1}$. This result is much higher than the Λ of polycrystalline ScN thin films ($5.5\text{--}12.3 \text{ W m}^{-1} \text{ K}^{-1}$)²⁹ and epitaxial layers ($12.3\text{--}20.7 \text{ W m}^{-1} \text{ K}^{-1}$).^{5,29,40} Such high values of Λ result from a large electronic thermal conductivity (Λ_e) in the ScN samples due to the high carrier concentrations. We estimate Λ_e from the Wiedemann-Franz law $\Lambda_e = LT/\rho$, where L is the Lorenz number ($2.44 \times 10^{-8} \text{ W } \Omega \text{ K}^{-2}$), ρ is the electrical resistivity, and T is the absolute temperature. Taking the room temperature value of $\rho = 39 \mu\Omega \text{ cm}$ from the Hall resistivity measurement, then the Λ_e is estimated to be $19 \text{ W m}^{-1} \text{ K}^{-1}$. Then from $\Lambda_{\text{ph}} = \Lambda - \Lambda_e$, the phonon thermal conductivity (Λ_{ph}) of ScN is approximately $35 \text{ W m}^{-1} \text{ K}^{-1}$.⁴¹ This result is relatively high compared with the Λ_{ph} of common transition metal nitrides and carbides.^{41,42} However, the measured Λ_{ph} in ScN is lower than the prediction from the first-principles based Boltzmann transport equation calculation, $51.5 \text{ W m}^{-1} \text{ K}^{-1}$.⁴³ This result is not surprising since the high impurity concentrations (N_A and N_D) as well as the resultant high carrier concentration could lead to strong scattering

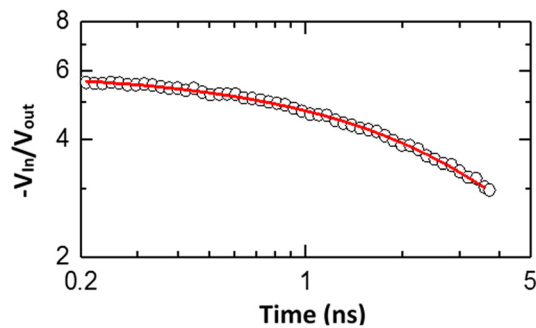


FIG. 3. Representative experimental data (black open circles) and model fitting curve (red solid line) of the thermal conductivity measurement by TDTR.

of phonons, limiting Λ_{ph} .⁴⁴ Our result shows that the Λ_{ph} reported in another first-principles based calculation, $20 \text{ W m}^{-1} \text{ K}^{-1}$,²⁹ might be an underestimation of the intrinsic value.

In conclusion, high quality bulk ScN single crystals with good electrical and thermal properties was grown by physical vapor transport. The growth of such thick layers enables threading dislocations to combine and annihilate, resulting in a much lower defect density than is possible in thin films. For example, Mathis *et al.*⁴⁵ estimated that the dislocation density in GaN is reduced by three orders of magnitude as the layer thickness increases from $1 \mu\text{m}$ to 1 mm . A similar reduction is anticipated here for ScN. Hall-effect measurements showed that ScN crystals were *n*-type with a high carrier concentration, yet with an electron mobility reasonably high in comparison to ScN thin films produced by deposition. The high room temperature thermal conductivity of PVT ScN also suggests that it is of high quality.

Support for this project from the National Science Foundation Division of Materials Research Award No. 1508172 to KSU and No. 1800139 to WSU is greatly appreciated. This research was also supported by the Air Force Office of Scientific Research through Project No. FA9550-RY17COR490. The authors would like to thank T. A. Cooper for performing the Hall-effect measurements.

REFERENCES

- B. Saha, M. Garbrecht, J. A. Perez-Taborda, M. H. Fawey, Y. R. Koh, A. Shakouri, M. Martin-Gonzalez, L. Hultman, and T. D. Sands, *Appl. Phys. Lett.* **110**, 252104 (2017).
- H. A. Al-Britten, A. R. Smith, and D. Gall, *Phys. Rev. B* **70**, 045303 (2004).
- M. A. Moram, Z. H. Barber, C. J. Humphreys, T. B. Joyce, and P. R. Chalker, *J. Appl. Phys.* **100**, 023514 (2006).
- D. Gall, I. Petrov, N. Hellgren, L. Hultman, J. E. Sundgren, and J. E. Greene, *J. Appl. Phys.* **84**, 6034 (1998).
- P. V. Burmistrova, J. Maassen, T. Favaloro, B. Saha, S. Salamat, Y. Rui Koh, M. S. Lundstrom, A. Shakouri, and T. D. Sands, *J. Appl. Phys.* **113**, 153704 (2013).
- N. Turesson, N. Van Nong, D. Fournier, N. Singh, S. Acharya, S. Schmidt, L. Belliard, A. Soni, A. L. Febvrier, and P. Eklund, *J. Appl. Phys.* **122**, 025116 (2017).
- S. Kerdongpanya, N. Van Nong, N. Pryds, A. Žukauskaitė, J. Jensen, J. Birch, J. Lu, L. Hultman, G. Wingqvist, and P. Eklund, *Appl. Phys. Lett.* **99**, 232113 (2011).
- S. Kerdongpanya, B. Alling, and P. Eklund, *Phys. Rev. B* **86**, 195140 (2012).
- M. Garbrecht, B. Saha, J. L. Schroeder, L. Hultman, and T. D. Sands, *Sci. Rep.* **7**, 46092 (2017).
- A. Herwadkar and W. R. L. Lambrecht, *Phys. Rev. B* **72**, 235207 (2005).

- ¹¹R. Matloub, M. Hadad, A. Mazzalai, N. Chidambaram, G. Moulard, C. S. Sandu, T. Metzger, and P. Muralt, *Appl. Phys. Lett.* **102**, 152903 (2013).
- ¹²F. Tasnadi, B. Alling, C. Höglund, G. Wingqvist, J. Birch, L. Hultman, and I. A. Abrikosov, *Phys. Rev. Lett.* **104**, 137601 (2010).
- ¹³M. A. Moram, Y. Zhang, M. J. Kappers, Z. H. Barber, and C. J. Humphreys, *Appl. Phys. Lett.* **91**, 152101 (2007).
- ¹⁴M. A. Moram, M. J. Kappers, and C. J. Humphreys, *Phys. Status Solidi C* **7**, 1778 (2010).
- ¹⁵C. Constantin, H. Al-Brithen, M. B. Haider, D. Ingram, and A. R. Smith, *Phys. Rev. B* **70**, 193309 (2004).
- ¹⁶R. Deng, P. Y. Zheng, and D. Gall, *J. Appl. Phys.* **118**, 015706 (2015).
- ¹⁷Y. Kumagai, N. Tsunoda, and F. Oba, *Phys. Rev. Appl.* **9**, 034019 (2018).
- ¹⁸J. S. Cetnar, A. N. Reed, S. C. Badescu, S. Vangala, H. A. Smith, and D. C. Look, *Appl. Phys. Lett.* **113**, 192104 (2018).
- ¹⁹S. W. King, R. F. Davis, and R. J. Nemanich, *J. Vac. Sci. Technol., A* **32**, 061504 (2014).
- ²⁰H. Al-Brithen and A. R. Smith, *Appl. Phys. Lett.* **77**, 2485 (2000).
- ²¹Y. Oshima, E. G. Villora, and K. Shimamura, *J. Appl. Phys.* **115**, 153508 (2014).
- ²²G. Harbecke, E. Meier, and J. P. Dismukes, *Opt. Commun.* **4**, 335 (1972).
- ²³B. Saha, G. Naik, V. P. Drachev, A. Boltasseva, E. E. Marinero, and T. D. Sands, *J. Appl. Phys.* **114**, 063519 (2013).
- ²⁴J. P. Dismukes, W. M. Yim, and V. S. Ban, *J. Cryst. Growth* **13**, 365 (1972).
- ²⁵J. M. Gregoire, S. D. Kirby, G. E. Scopelios, F. H. Lee, and R. B. van Dover, *J. Appl. Phys.* **104**, 074913 (2008).
- ²⁶T. Ohgaki, I. Sakaguchi, N. Ohashi, and H. Haneda, *J. Cryst. Growth* **476**, 12 (2017).
- ²⁷J. Casamento, J. Wright, R. Chaudhuri, H. Xing, and D. Jena, *Appl. Phys. Lett.* **115**, 172101 (2019).
- ²⁸A. R. Smith, H. A. H. Al-Brithen, D. C. Ingram, and D. Gall, *J. Appl. Phys.* **90**, 1809 (2001).
- ²⁹S. Kerdsongpanya, O. Hellman, B. Sun, Y. K. Koh, J. Lu, N. Van Nong, S. I. Simak, B. Alling, and P. Eklund, *Phys. Rev. B* **96**, 195417 (2017).
- ³⁰H. A. Al-Atabi, N. Khan, E. Nour, J. Mondoux, Y. Zhang, and J. H. Edgar, *Appl. Phys. Lett.* **113**, 122106 (2018).
- ³¹H. A. Al-Atabi, Z. F. Al-Auda, B. Padavala, M. Craig, K. Hohn, and J. H. Edgar, *Cryst. Growth Des.* **18**, 3762 (2018).
- ³²L. Du, J. H. Edgar, E. A. Kenik, and H. Meyer, *J. Mater. Sci.* **21**, 78 (2010).
- ³³D. G. Cahill, *Rev. Sci. Instrum.* **75**, 5119 (2004).
- ³⁴K. Kang, Y. K. Koh, C. Chiritescu, X. Zheng, and D. G. Cahill, *Rev. Sci. Instrum.* **79**, 114901 (2008).
- ³⁵S. Li, Q. Zheng, Y. Lv, X. Liu, X. Wang, P. Y. Huang, D. G. Cahill, and B. Lv, *Science* **361**, 579 (2018).
- ³⁶Q. Zheng, S. Li, C. Li, Y. Lv, X. Liu, P. Y. Huang, D. A. Broido, B. Lv, and D. G. Cahill, *Adv. Funct. Mater.* **28**, 1805116 (2018).
- ³⁷B. Saha, J. Acharya, T. D. Sands, and U. V. Waghmare, *J. Appl. Phys.* **107**, 033715 (2010).
- ³⁸D. C. Look, *Electrical Characterization of GaAs Materials and Devices* (Wiley, New York, 1989), Chap. 1.
- ³⁹D. C. Look, K. D. Leedy, L. Vines, B. G. Svensson, A. Zubiaga, F. Tuomisto, D. R. Doutt, and L. J. Brillson, *Phys. Rev. B* **84**, 115202 (2011).
- ⁴⁰B. Saha, J. A. Perez-Taborda, J.-H. Bahk, Y. R. Koh, A. Shakouri, M. Martin-Gonzalez, and T. D. Sands, *Phys. Rev. B* **97**, 085301 (2018).
- ⁴¹Q. Zheng, A. B. Mei, M. Tuteja, D. G. Sangiovanni, L. Hultman, I. Petrov, J. E. Greene, and D. G. Cahill, *Phys. Rev. Mater.* **1**, 065002 (2017).
- ⁴²W. S. Williams, *JOM* **50**, 62 (1998).
- ⁴³C. Li and D. Broido, *Phys. Rev. B* **95**, 205203 (2017).
- ⁴⁴P. G. Klemens, *Proc. Phys. Soc. Sect. A* **68**, 1113 (1955).
- ⁴⁵S. K. Mathis, A. E. Romanov, L. F. Chen, G. E. Beltz, W. Pompe, and J. S. Speck, *J. Cryst. Growth* **231**, 371 (2001).